Polymer Journal, Vol. 36, No. 3, pp. 265—269 (2004)

SHORT COMMUNICATIONS

Study of Nanorheology and Nanotribology by Coarse-grained Molecular Dynamics Simulation

Hiroshi MORITA,*,† Takayuki IKEHARA,* Toshio NISHI,** and Masao DOI***

Japan Science and Technology Agency, Department of Computational Science and Engineering, Nagoya University, Chikusa-ku, Nagoya 464-8603, Japan
**Department of Applied Chemistry, School of Engineering, Kanagawa University, 3-27-1, Rokkakubashi, Kanagawa-ku, Yokohama 221-8686, Japan*
***Department of Organic and Polymeric Materials, Tokyo Institute of Technology, 2-12-1, Ohokayama, Meguro-ku, Tokyo 152-8552, Japan*
****Department of Computational Science and Engineering, Nagoya University, Chikusa-ku, Nagoya 464-8603, Japan*

(Received July 25, 2003; Accepted January 5, 2004)

KEY WORDS Coarse-grained Molecular Dynamics Simulation / Polymer Surface / OCTA / Atomic Force Microscopy /

Recently, physical properties at polymer surfaces have been paid much attention and many studies have been reported.[1–5] Atomic force microscopy (AFM) which measures the force acting on the AFM tips is one of the best tools to observe the properties in nano-order scale such as the change of the glass transition temperature near the surface region.[3–5] Nakajima *et al.*[1] measured the force–distance curve for a series of indentation-retraction movement of AFM tip for a surface of polymer changing the scanning rate of the indentation-retraction motion. In the case of slow scanning, they observed that in the retraction process there is a pulling force acting between the tip and the sample at an unexpected long distance. They conjectured that this force is caused by the pulling of the chain bridging between the tip and the sample. Terada *et al.*[2] have studied the nanotribology of a surface of polymer blend. They explained that the change of the friction force is due to the local configuration changes such as mound formation.

To confirm these conjectures and to see the actual molecular process in these experiments, we conducted molecular dynamics for nanorheology and nanotribology using the coarse-grained molecular dynamics simulation program COGNAC in OCTA system.[6] We developed a convenient method to construct the model surface using the self consistent field theory, and performed the simulations to analyze both indentation-retraction and friction processes of AFM tip.

As a model for MD simulation, we use the bead-spring model of Grest and Kremer.[7,8] Polymers consist of 100 beads connected by the following potential $U_{\mathrm{bond}}(r)$

$$U_{\mathrm{bond}}(r) = U_{\mathrm{FENE}}(r) + U_{\mathrm{LJbond}}(r)$$

$$U_{\mathrm{FENE}}(r) = \begin{cases} -\dfrac{1}{2}kR_0^2 \ln\left(1 - \left(\dfrac{r}{R_0}\right)^2\right), & (r \le R_0) \\ \infty, & (r > R_0) \end{cases}$$

$$U_{\mathrm{LJbond}}(r) = \begin{cases} 4\varepsilon\left[\left\{\left(\dfrac{\sigma}{r}\right)^{12} - \left(\dfrac{\sigma}{r}\right)^{6}\right\} + \dfrac{1}{4}\right], & (r \le 2^{1/6}\sigma) \\ 0, & (r > 2^{1/6}\sigma) \end{cases}$$

where k is the spring constant, and R_0 is the maximum extension of the spring. In our simulations, the parameters of k and R_0 are set to the same values of Kremer *et al.* $k = 30.0\varepsilon/\sigma^2$ and $R_0 = 3.0\sigma$. (σ and ε mean the Lennard–Jones diameter and Lennard–Jones energy, respectively.)

†To whom correspondence should be addressed (E-mail: hmorita@stat.cse.nagoya-u.ac.jp).

The AFM tip is represented by a sphere the radius of which is 4 times larger than that of polymer segments. The non-bonding interaction between the polymer segments and that between the polymer segments and the tip are assumed to be given by the following Lennard–Jones potential:

$$U_{ij}^{\mathrm{LJ}}(r) = \begin{cases} 4\varepsilon_{ij}\left[\left\{\left(\frac{\sigma_{ij}}{r}\right)^{12} - \left(\frac{\sigma_{ij}}{r}\right)^{6}\right\} - \left\{\left(\frac{\sigma_{ij}}{r^{\mathrm{cut}}}\right)^{12} - \left(\frac{\sigma_{ij}}{r^{\mathrm{cut}}}\right)^{6}\right\}\right], & (r \le r^{\mathrm{cut}}) \\ 0, & (r > r^{\mathrm{cut}}) \end{cases}.$$

The parameters, $\varepsilon_{\mathrm{PX}}$, σ_{PX}, and $r_{\mathrm{PX}}^{\mathrm{cut}}$ (where X stands for polymer (P) or tip (T)) are set as follows; $\varepsilon_{\mathrm{PP}} = 1.0\varepsilon$, $\sigma_{\mathrm{PP}} = 1.0\sigma$, $r_{\mathrm{PP}}^{\mathrm{cut}} = 2.0\sigma$, $\varepsilon_{\mathrm{PT}} = 1.5\varepsilon$, $\sigma_{\mathrm{PT}} = 4.0\sigma$, and $r_{\mathrm{PT}}^{\mathrm{cut}} = 6.0\sigma$. These parameters indicate that the AFM tip attracts the beads of polymer. If we use smaller value of $\varepsilon_{\mathrm{PT}}$, such as $\varepsilon_{\mathrm{PT}} = 1.0\varepsilon$, the attraction between the AFM tip and the polymer is not clearly observed. The condition of $\varepsilon_{\mathrm{PT}} > \varepsilon_{\mathrm{PP}}$ is important for our model. The above set of parameters for the polymers are the same as that used by Grest and Kremer[7,8] except for the cut off radius: Grest and Kremer used the $r_{\mathrm{PP}}^{\mathrm{cut}} = 2.5\sigma$, but the calculation of the bulk system indicates that this does not effect the diffusivity seriously.[9]

For the equation of motion of beads, we used the Langevin equation,

$$m\frac{d^2\mathbf{r}_n}{dt^2} = \mathbf{F}_n - \Gamma\frac{d\mathbf{r}_n}{dt} + \mathbf{W}_n(t)$$

where m is the mass of the bead, $\mathbf{F}_n$ is the force acting on the bead n, Γ is the friction constant, and $\mathbf{W}_n(t)$ is a Gaussian white noise which is generated according to the following equation.

$$\langle \mathbf{W}_n(t)\mathbf{W}_m(t')\rangle = 2k_{\mathrm{B}}Tm\Gamma\delta_{nm}\mathbf{I}\delta(t-t')$$

In our simulation, $k_{\mathrm{B}}T$ is set to 0.4ε, Γ is $0.5\tau^{-1}$, where τ is the unit of time given by $\sigma(m/\varepsilon)^{1/2}$. The AFM tip is moved with the constant velocity either normal to the surface (indentation) or parallel to the surface (friction). The tip velocity was taken to be $v = 0.01\sigma/\tau$.

We now discuss how there simulation condition corresponds to the real situation of polystyrene film following the same argument of Kremer and Grest.[8] The simulation parameters used in our simulations are same as those of Grest and Kremer[7,8] except for $r_{\mathrm{PP}}^{\mathrm{cut}}$. The following correspondence gives an indication of the order of the experimental system.

(i) The diameter of the AFM: Kremer and Grest discussed σ corresponds to 1.26 nm. Here the diameter of our tip is about 10 nm, which is the same order of the diameter of the real tip head (20–30 nm).

(ii) The scanning rate: The scanning rate of the indentation-retraction process in our simulation is about 1.6×10^4 Hz. The scanning rate in the experiment is the order of 0.1–1 Hz. Therefore, the scanning rate of our simulation is much faster than the experimental one. From our another simulations for the bulk system at $T = 0.5$, the entanglement time τ_{e} is calculated as about 5000τ,[9] and the total time for the indentation-retraction simulations is shorter than τ_{e} (2000τ).

(iii) Molecular weight: Kremer and Grest reported that the entanglement length of the model chain is about $N_{\mathrm{e}} \cong 35$.[7,8] The length of our model chain ($N = 100$) is 3 times longer than the entanglement molecular weight. Thus the entanglement molecular weight corresponds to $M_{\mathrm{e}} = 18000$.

(iv) Temperature: To obtain the relationship between the simulation temperature and the real temperature, we performed the simulations for the bulk polymer system of 100 chains with 100 beads using the NPT ensemble (control of the pressure by Andersen[10] and that of the temperature by Grest and Kremer[7,8]), and found that the temperature dependence of the density shows a break at about $T = 0.4\varepsilon/k_{\mathrm{B}}$. Thus our simulation was done near the glass transition temperature, which is about 400 K for PS.

In this study, the molecular configuration near the surface was constructed using the density biased Monte Carlo (DBMC) method developed by Aoyagi *et al.*[11,12] In the DBMC, the segment density is first calculated by the self consistent field (SCF) method,[13–15] and then beads-spring chains are placed under the restriction of density weight as a function of chain length and position which is obtained by SCF simulation. To obtain the surface structure using SCF simulation,[16,17] we performed 1-dimensional SCF simulations (system size: 32) for the blend system composed of both void and polymer with 100 segments. The Flory's interaction parameter (χ) between the void and the polymer segment is set as $\chi = 1.0/(k_{\mathrm{B}}T)$ in order to simulate the segregation of the end segments at the surface. At the case of $\chi = 1.0$, 1.5, and 3.0, we can observe this segregation and the sharp interface. Half of interfacial width between void and polymer is less than 2 layer. From the experimental results, the roughness of the film surface obtained by spin cast is the order of 0.1–1.0 nm, and

the interfacial width by the SCF simulations is not far from the experimental one. Using the result of the SCF simulation, we constructed the initial guess for MD simulation composed of 100 or 400 chains having 100 beads using DBMC method. In the MD simulations, the void particle is not included, and this system realizes the experiments under the vacuum condition. In this method, the one length of the polymer in the SCF simulation corresponds to the one bead in MD simulation, and the system size in the depth direction for MD simulation is 32, which is the same as that in the SCF simulation. The structure was then relaxed using MD simulations, and the relaxation was checked by the total energy.

Figure 1 shows the segment density and the fraction of the end segments plotted against the coordinate normal to the surface z. Figure 1a shows the SCF result and Figure 1b shows that obtained by the MD simulations. The actual structure of the 100 chains is shown in Figure 2a. It is seen that the density profile and the end segment distribution obtained by the MD simulation is in reasonable agreement with those of

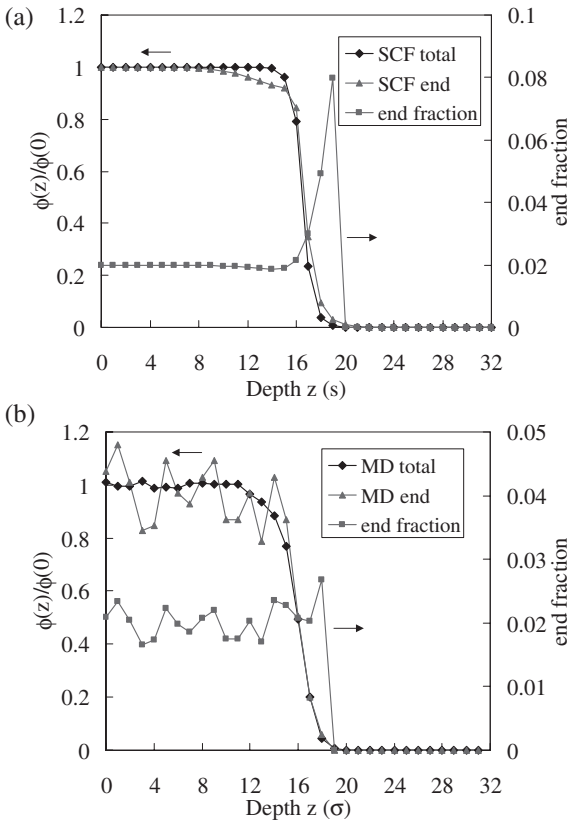

Figure 1. Depth profile of the total density and the end segment density obtained by SCF and MD simulations. Plotted densities are averaged one at each depth regions. Both total and end segment densities are normalized by the averaged density at position $z = 0$–3. End fraction is the value of the end segment density divided by the total density. In the case that the end segment density is smaller than 10^{-4}, this fraction is set to zero.

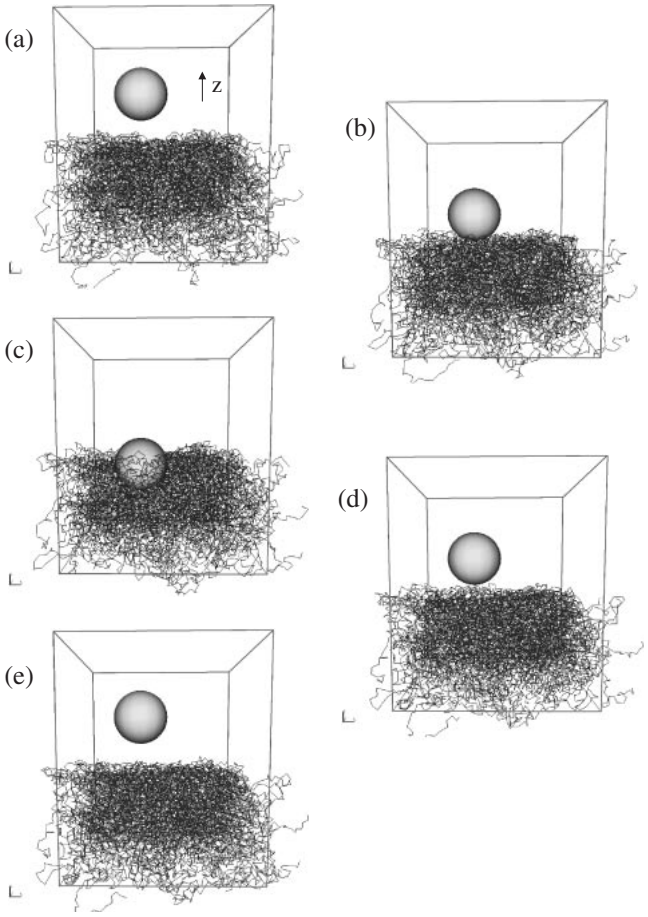

Figure 2. Snap shot structures of the MD simulation at the indentation-retraction process. Indentation and retraction processes correspond to a–c and c–e, respectively.

SCF results. The agreement is not perfect as the parameter optimization for MD simulation was not done. The profile of the end fraction shown in Figures 1a and b indicates the enrichment of the chain end group at the surface. This is in agreement with the previous experimental results.[3,18]

Figure 2 shows the results of MD simulations for the indentation-retraction process at the temperature near T_g. Figure 2a to 2c shows the structural change in the indentation process and Figure 2c to 2e shows that of the retraction process. The force acting on the AFM tip sphere is plotted against z in Figure 3. Minus value of the force means the attractive force between the AFM tip and polymer surface. This curve can be compared with the force–distance curve obtained by experiments. Note that the force–distance curve obtained by experiments includes the effect of the rigidity of the cantilever, which is not included in our simulation. We checked that the shape of the curves are not changed significantly even if include the spring effect of tip as a correction.

Figures 2 and 3 indicate the following molecular process for the nano-indentation and retraction experiments. As the AFM tip approaches the polymer sur-

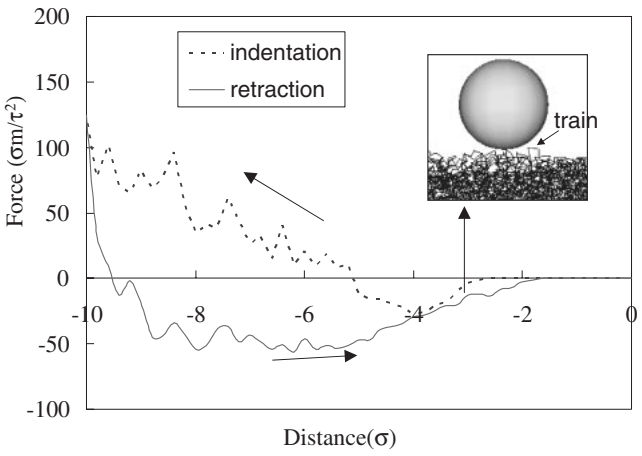

Figure 3. Force–distance curve obtained by MD simulation. Inset shows the magnified one at the contact region of Figure 2d. The horizontal and vertical axes mean the depth direction (z) of the AFM tip sphere and the vertical force acting on the tip. The arrow means the traveling direction of tip.

face a weak attractive force is observed. This is due to the van der Waals attraction between the AFM tip and the polymer surface. As the AFM tip is pushed into the polymer surface, the force becomes repulsive which increases as the tip is pushed further. Note that the surface around the AFM tip does not move up as it should if the polymer is an incompressible liquid. Thus the polymer is behaving as an elastic solid in this case. The repulsive force is due to the densification of polymer segments in the region of the tip front. The fluctuation in the force curve reflects the thermal motion of the surrounding polymer segments.

In the retraction process, the repulsive force becomes smaller and changes to attractive. The inset of Figure 3 shows the magnified figure of the contact region at the position indicated in the figure. It is seen that the chains interacting with the tip form train conformation, which is similar to the adsorbed chain at a surface.[15] As the tip sphere is pulled further, the polymer detach from the surface and the force finally becomes zero. It is clear that the long lasting attractive force is due to the "fishing up of the polymer chains" since the position where the attractive force becomes zero in the retraction process is above the position at which the attractive force starts to appear in the indentation process. Our result of the force-distance curve is similar to that of experiments near T_g. (For example Figure 2b in Ref 1.)

Next, we study the friction force process. The simulation of friction process was realized by moving the tip in the lateral direction. To simulate this process, a larger width of the surface is needed. We constructed the surface using 400 chains each consisting of 100 beads, and the size of the lateral direction was twice as large as the former indentation simulations. The

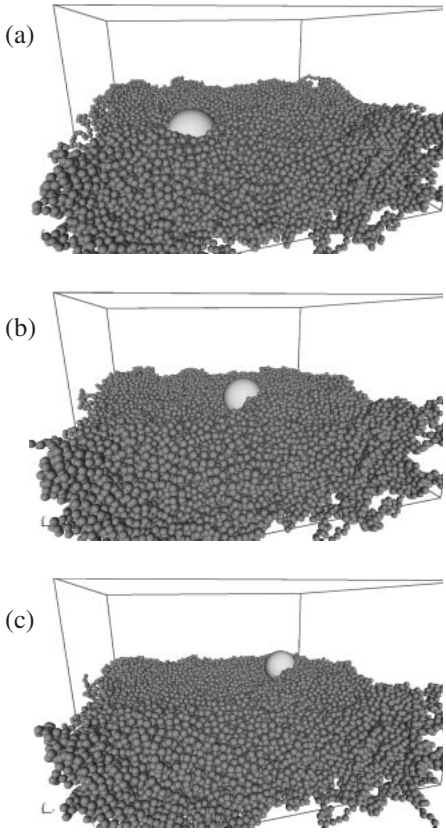

Figure 4. Snap shot structures of the MD simulation at the friction process.

simulation for the indentation process was performed at first, and then the tip was moved to the lateral direction with the constant velocity $v = (\pm 0.07071068\sigma/\tau, \pm 0.07071068\sigma/\tau, 0)$. In the simulations for friction process, the height (z position) of the tip was always fixed.

Figure 4 shows the results of MD simulations for friction process. In Figure 4, the friction process proceeds from a to c. Initial structure in Figure 4a is obtained from the indentation simulation, in which the indentation depth of the tip is about 6σ. We performed the two and half of the forward and backward processes of tip movements. Figure 5 shows the lateral force acting on the tip in the two loops of forward and backward processes. The plus value of the force means the force in the forth direction at first time. This curve corresponds to the friction loop observed in the experiments. (For example Figure 3 in Ref 2.) Our result of the friction loop curve is quite similar to the experimental one. We will analyze the dynamics of the contacted chains with tip in the friction process, and the details will be discussed in the latter papers.[9]

In this paper, we report the surface mechanical study of polymer system in nano-order scale using OCTA. We proposed a convenient method of constructing the initial structure of the beads-spring chains, which can reproduce the surface enrichment

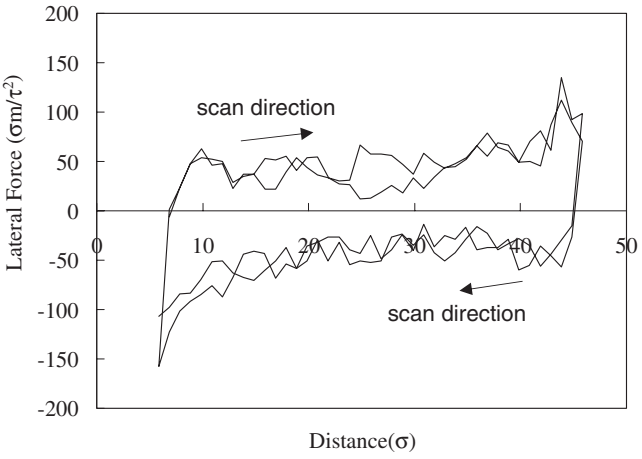

Figure 5. Friction loop curve obtained by MD simulation. The horizontal and vertical axes mean the lateral distance of the traveling tip and the lateral force acting on the tip. The arrow means the moving direction of tip. The force plotted in this figure is in the two loops of forward and backward processes.

of the chain end group. Using this surface, we can simulate the force–distance and the friction loop curves, which correspond to the experimental ones.

Acknowledgment. The authors would like to thank Prof. Kohzo Ito, Prof. Jyun-ichi Takimoto, and Prof. Toshihiro Kawakatsu for many helpful comments and discussions. This work is financially supported by the Japan Science and Technology Agency (JST), the New Energy and Industrial Technology Development Organization (NEDO), and the Ministry of Education, Culture, Sports, Science and Technology, Japan.

REFERENCES

1. K. Nakajima, H. Yamaguchi, J. C. Lee, M. Kageshima, T. Ikehara, and T. Nishi, *Jpn. J. Appl. Phys.*, **36**, 3850 (1997).
2. Y. Terada, M. Harada, T. Ikehara, and T. Nishi, *J. Appl. Phys.*, **87**, 2803 (2000).
3. T. Kajiyama, K. Tanaka, and A. Takahara, *Macromolecules*, **30**, 280 (1997).
4. T. Kajiyama, K. Tanaka, N. Satomi, and A. Takahara, *Macromolecules*, **31**, 5150 (1998).
5. K. Tanaka, A. Takahara, and T. Kajiyama, *Macromolecules*, **33**, 7588 (2000).
6. http://octa.jp
7. G. S. Grest and K. Kremer, *Phys. Rev. A*, **33**, 3628 (1986).
8. K. Kremer and G. S. Grest, *J. Chem. Phys.*, **92**, 5057 (1990).
9. H. Morita, T. Ikehara, T. Nishi, and M. Doi, in preparation.
10. H. C. Andersen, *J. Chem. Phys.*, **72**, 2384 (1980).
11. T. Aoyagi, F. Sawa, T. Shoji, H. Fukunaga, J. Takimoto, and M. Doi, *Comput. Phys. Commun.*, **145**, 267 (2002).
12. T. Aoyagi, J. Takimoto, and M. Doi, *J. Chem. Phys.*, **117**, 8153 (2002).
13. E. Helfand and Z. R. Wasserman, *Macromolecules*, **9**, 879 (1976).
14. M. W. Matsen and M. Schick, *Phys. Rev. Lett.*, **72**, 2660 (1994).
15. G. J. Fleer, M. A. Cohen Stuart, J. M. H. M. Scheutjens, T. Cosgrove, and B. Vincent, "Polymers at Interfaces," Chapman & Hall, London, 1993.
16. A. Hariharan, S. K. Kumar, and T. P. Russell, *J. Chem. Phys.*, **98**, 6516 (1993).
17. H. Morita, T. Kawakatsu, and M. Doi, *Macromolecules*, **34**, 8777 (2001).
18. W. L. Wu, W. J. Orts, J. H. van Zanten, and B. M. Fanconi, *J. Polym. Sci., Part B: Polym. Phys.*, **32**, 2475 (1994).